Deciphering the NMR Fingerprints of the Disordered System with Quantum Chemical Studies

Yan Ling and Yong Zhang*

Department of Chemistry and Biochemistry, University of Southern Mississippi, 118 College Drive No. 5043, Hattiesburg, Mississippi 39406

Received: January 6, 2009; Revised Manuscript Received: March 5, 2009

Recent developments in solid-state NMR techniques helped acquire high-resolution NMR spectra for solid systems with structural disorder. But the structural origin of the observed chemical shift nonequivalence in these systems has not been revealed. We report a quantum chemical investigation of the solid-state NMR spectrum in *N*,*N*-bis(diphenylphosphino)-*N*-((*S*)-α-methylbenzyl)amine, where eight nonequivalent ^{31}P NMR chemical shifts were resolved with a range of 13.0 ppm. Results from using different quantum chemical methods, computational algorithms, intermolecular effects, and structures indicate that for the disordered system, geometry optimization gives the best accord with experimental NMR chemical shifts, which has a theory-versus-experiment correlation $R^2 = 0.949$ and SD = 1.1 ppm, or $R^2 = 0.994$ and SD = 0.4 ppm when the average of two unassigned NMR shifts for each molecule is used. In addition, these calculations indicate that the experimental chemical shift nonequivalence in this system is mainly a consequence of the different geometries around the phosphorus atoms due to disordered environments. The experimental ^{31}P NMR chemical shifts are well correlated ($R^2 = 0.981$) with two conformation angles and one bond length, each associated with one of the three bonding interactions around the phosphorus atoms. These results will facilitate the use of quantum chemical techniques in structural characterization of disordered solids and elucidation of NMR properties.

Introduction

NMR spectroscopy is a powerful technique that can provide fingerprints of molecular and biomolecular structures as well as the associated structural changes. Recent developments in solid-state NMR spectroscopy have advanced these studies to many disordered solid systems, such as fibrils of proteins,[1,2] protein−peptidoglycan complexes,[3] cellulose,[4,5] silicates,[6] polymers,[7] and glasses,[8] as well as structural disorder in crystalline solids.[4,5] Different NMR chemical shifts were observed for the same molecules in the different environments in the disordered systems, producing the so-called chemical shift nonequivalence. Previous investigations of proteins and relevant peptides indicate that numerous specific structural information can be extracted from the NMR chemical shift nonequivalence when quantum chemical methods were used.[9−12] However, little work has been done in the quantum chemical investigations of NMR chemical shifts in disordered solids.[6] In particular, there are no quantum chemical investigations reported to disclose the structural origins of the NMR chemical shift nonequivalence in disordered solids. Since many chemical and biochemical systems have disordered structures and high-resolution NMR spectra can now be acquired for these systems, it will be useful to decipher these NMR fingerprints to obtain specific structural information through the assistance of quantum chemical investigations, which should facilitate structural characterizations of these systems.

In this paper, we report a quantum chemical investigation of the solid-state ^{31}P NMR spectrum of *N*,*N*-bis(diphenylphosphino)-*N*-((*S*)-α-methylbenzyl)amine.[4,5] As shown in Figure 1A, there are four molecules in a crystal structural unit and each molecule has two different phosphorus atoms.[13] It is interesting to note that all of these eight phosphorus atoms experience different environments, which can now be resolved by using advanced solid-state NMR techniques developed recently.[4,5] These NMR shifts exhibit an experimental range of 13.0 ppm in the high-resolution spectrum. This range is comparable to those seen with solid-state ^{13}C NMR shifts of amino acids in peptides and proteins investigated previously by using quantum chemical methods,[10−12] which suggests that a quantum chemical investigation of these ^{31}P NMR experimental data may also be able to determine the structural origin of this observed chemical shift nonequivalence. Results from a comprehensive set of calculations with a variety of quantum chemical methods, NMR computational formalisms, and approaches to account for intermolecular interactions suggest that geometry optimization is required to enable best accord with experiment (the theory-versus-experiment correlation coefficient is $R^2 = 0.95$ with SD = 1.1 ppm). In addition, excellent correlations between the experimental NMR chemical shifts and local geometric parameters were found with $R^2 = 0.98$.

Computational Details

Each of the four molecules in the crystal structural unit (Figure 1A) was calculated and in all calculations, the complete molecular structure of *N*,*N*-bis(diphenylphosphino)-*N*-((*S*)-α-methylbenzyl)amine consisting of 64 atoms was used, as shown in Figure 1B. The 6-311++G(2d,2p) basis for all atoms was employed based on previous investigations of ^{31}P NMR chemical shifts,[14,15] resulting in 1251 basis functions for each molecule. To calculate ^{31}P NMR chemical shielding properties, both ab initio Hartree−Fock (HF) and density functional theory (DFT-B3LYP[17,18]) methods were used, together with two NMR computational formalisms: gauge-independent atomic orbital

* To whom correspondence should be addressed.

10.1021/jp9001324 CCC: $40.75
Published on Web 03/30/2009

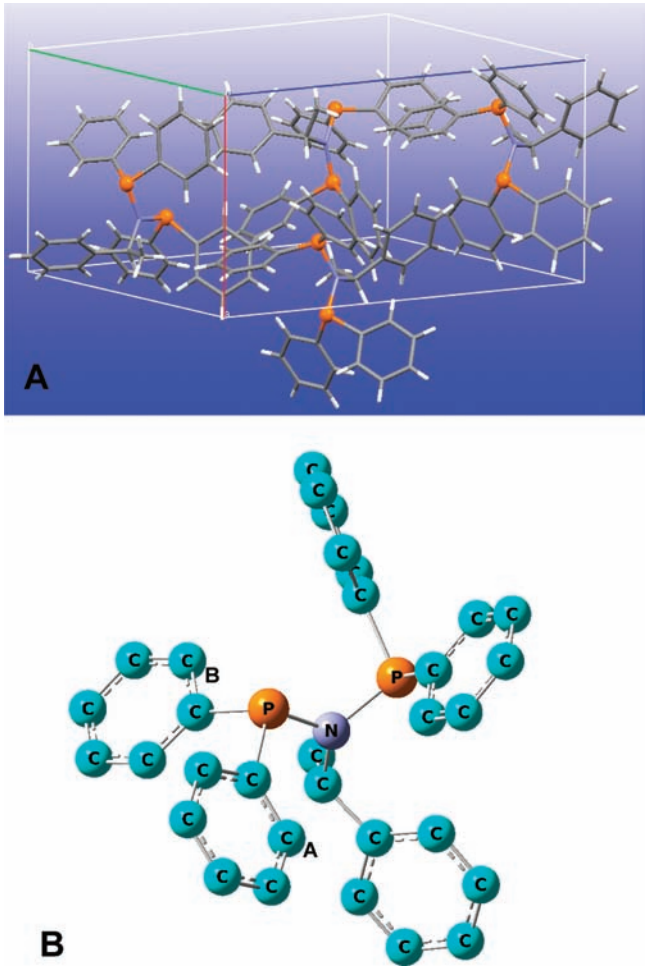

Figure 1. (A) The crystal structure of *N*,*N*-bis(diphenylphosphino)-*N*-((*S*)-α-methylbenzyl)amine (P, orange ball; C, gray; N, blue; H, white) and (B) its molecular structure with hydrogen atoms omitted for clarity.

(GIAO)[19] and the continuous set of gauge transformations (CSGT)[20] methods as implemented in Gaussian 03 and Gaussian 98 programs.[21,22] Additional calculations incorporating a large range of intermolecular effects were also carried out by using two different theoretical treatments. One uses the charge field perturbation (CFP) approach[23,24] as described in ref 14, which basically employs a large charge lattice placed in positions based on crystal structure symmetry to simulate the environment around the central molecule of interest. This CFP approach was found to effectively improve the predictions of ^{31}P NMR shifts in some compounds.[14,15] The other way to account for the environmental effect is to use a "solvent" model with the self-consistent reaction field (SCRF) method with the PCM formalism[25−29] in the Gaussian 03 program, as used previously in NMR chemical shift predictions.[12]

In addition to the above calculations with the experimental X-ray structure for *N*,*N*-bis(diphenylphosphino)-*N*-((*S*)-α-methylbenzyl)amine,[13] another set of calculations were also done with partial geometry optimizations of phosphorus atoms and their directly bonded atoms. To facilitate the geometry optimization calculations, a locally dense basis set scheme was used, with the 6-31G(d), 6-311G(d), and 6-311G(2d) basis sets used for the phosphorus atoms and their directly bonded atoms in respective calculations, while the remaining atoms in the molecules were treated with a 6-31G(d) basis. This is basically the approach used previously to evaluate ^{31}P NMR chemical shifts in some other phosphorus-containing compounds.[15] Regarding the geometry optimization methods, in addition to the hybrid HF-DFT method B3LYP and mPW1PW91,[30,31] we also investigated a couple of pure DFT methods in the Gaussian 03 program. One is BVWN5 with the Becke exchange functional[32] and VWN5 correlation functional,[33] and the other is mPWVWN with the modified Perdew−Wang 1991 (mPW) exchange functional[30] and VWN correlation functional.[33]

Since the absolute values of experimental ^{31}P NMR chemical shieldings cannot be well reproduced directly from the calculated ^{31}P NMR chemical shieldings (σ^{calc}),[14,15] the predicted ^{31}P NMR chemical shifts (δ^{calc}) were computed from the linear regression between the calculated ^{31}P NMR chemical shieldings (σ^{calc}) and the experimental NMR chemical shifts (δ^{expt}), as done before.[14,15]

Results and Discussion

The computed ^{31}P NMR chemical shifts (δ^{calc}) together with the corresponding experimentally[5] measured chemical shifts (δ^{expt}) are listed in Table 1, while the computed ^{31}P NMR chemical shieldings (σ^{calc}) are presented in Table S1 in the Supporting Information. Consistent with the experimental observation of eight different ^{31}P NMR shifts for the eight phosphorus atoms in the crystal structural unit, all our computational results showed eight distinguishable shifts, as shown in Table 1. The assignment of these shifts is based on both experimental NMR investigations showing four pairs of peaks in the spectrum for the four different molecules in the crystal unit (**1**, **1′**, **2**, **2′**, **3**, **3′**, **4**, **4′**) and the computational results to match lower chemical shielding with higher chemical shift.[14,15]

The first series of NMR calculations for this disordered system were performed with the use of the X-ray structure, as done previously in the quantum chemical investigations of ^{13}C and ^{31}P NMR chemical shifts in some ordered systems.[11,12,14,15] As shown in Table 1, using the GIAO NMR computational approach, the calculated ^{31}P NMR chemical shifts for these eight nonequivalent sites have a good correlation ($R^2 = 0.899$) with experimental values, when the previously used HF/6-311++G(2d,2p) method was used. The standard deviation is 1.6 ppm, which is not large, indicating that generally these calculations are good. This suggests that the X-ray structure is able to provide a good estimate of the experimental chemical shift nonequivalence. As shown in Table 2, the local bond lengths and angles around the phosphorus atoms are of small ranges, while the conformation angles of the phenyl rings that are attached to the phosphorus atoms ($\angle$N−P−C−C_A and $\angle$N−P−C−C_B; see an example in Figure 1B and definitions in the footnote of Table 2) have a large variation of ∼200°, showing a large disorder in this solid system. Consistent with this observation, no correlations between the experimental ^{31}P NMR shifts and local bond lengths/angles can be found, while there is a good correlation between the absolute sine values of these two angles and δ^{expt} values, with $R^2 = 0.880$.

However, these NMR shift predictions are still inferior to previous calculations of experimental ^{31}P NMR chemical shifts in other solid systems, which has a better correlation of $R^2 = 0.95$.[14] Additional calculations were also done by using this X-ray structure with the use of the B3LYP method that incorporates the electron correlation effect compared to the above used HF method, a couple of computational measures that take into account the environmental intermolecular effect using the charge field perturbation (CFP) approach[14,15,23,24] and a continuum model (SCRF),[12] and another NMR property computational algorithm CSGT method. But as shown in Table 1, no improvements were obtained. These results indicate that

TABLE 1: Experimental and Computed ^{31}P NMR Chemical Shifts (ppm)[a]

structure	method			**1**	**1′**	**2**	**2′**	**3**	**3′**	**4**	**4′**	R^2	SD
			δ^{expt}	47.3	50.5	51.0	56.7	55.8	60.3	57.0	57.5		
X-ray	GIAO	HF/6-311++G(2d,2p)	δ^{calc}	47.2	48.8	52.9	57.2	56.7	60.2	54.5	58.7	0.899	1.60
		B3LYP/6-311++G(2d,2p)	δ^{calc}	48.2	48.3	51.7	58.7	56.7	60.3	54.8	57.5	0.896	1.62
		HF/6-311++G(2d,2p) + CFP	δ^{calc}	47.3	48.2	53.3	57.5	56.4	60.1	54.4	58.8	0.871	1.83
		HF/6-311++G(2d,2p) + SCRF	δ^{calc}	47.2	48.8	52.9	57.4	56.5	60.3	54.2	58.8	0.889	1.68
	CSGT	HF/6-311++G(2d,2p)	δ^{calc}	47.3	48.6	53.1	57.0	56.6	60.4	54.3	58.9	0.883	1.73
		B3LYP/6-311++G(2d,2p)	δ^{calc}	46.8	48.8	53.3	57.5	56.8	60.0	54.4	58.5	0.884	1.73
		HF/6-311++G(2d,2p) + CFP	δ^{calc}	47.5	47.9	53.5	57.4	56.3	60.3	54.2	59.1	0.849	2.01
Opt: B3LYP/6-31G(d)	GIAO	HF/6-311++G(2d,2p)	δ^{calc}	48.4	49.5	51.2	56.4	55.3	61.5	55.3	58.5	0.945	1.15
Opt: B3LYP/6-311G(d)		HF/6-311++G(2d,2p)	δ^{calc}	48.3	49.6	51.4	56.3	55.1	61.7	55.2	58.6	0.938	1.23
Opt: mPW1PW91/6-31G(d)		HF/6-311++G(2d,2p)	δ^{calc}	48.0	49.8	51.8	55.9	55.0	62.0	54.8	58.9	0.916	1.45
Opt: BVWN5/6-311G(2d)		HF/6-311++G(2d,2p)	δ^{calc}	48.8	49.2	50.5	57.0	55.6	61.2	55.6	58.1	0.948	1.12
Opt: mPWVWN/6-311G(2d)		HF/6-311++G(2d,2p)	δ^{calc}	48.7	49.3	50.7	56.9	55.5	61.3	55.5	58.2	0.949	1.11

[a] The experimental NMR shifts and X-ray structure are from refs 5 and 13, respectively.

TABLE 2: ^{31}P NMR Chemical Shieldings and Geometric Parameters[a]

structure		σ^{calc} (ppm)	R_{P-N} (Å)	R_{P-C} (Å)	$R_{P-C'}$ (Å)	$^{av}R_{P-C}$ (Å)	∠C−P−C (deg)	^{av}∠N−P−C (deg)	∠N−P−C−C_A (deg)	∠N−P−C−C_B (deg)
X-ray	**1**	325.2	1.729	1.827	1.827	1.827	100.6	104.7	−82.6	−11.2
	1′	323.4	1.708	1.835	1.840	1.838	100.7	106.0	83.2	−11.2
	2	318.7	1.716	1.831	1.845	1.838	100.9	105.8	−87.7	−30.5
	2′	313.9	1.719	1.823	1.825	1.824	103.7	105.2	49.9	−118.2
	3	314.4	1.709	1.827	1.842	1.835	101.7	105.2	7.2	−76.5
	3′	310.5	1.727	1.830	1.841	1.836	100.8	103.2	25.5	79.3
	4	316.9	1.705	1.835	1.841	1.838	99.8	105.3	2.8	−74.7
	4′	312.1	1.732	1.823	1.838	1.831	101.4	104.9	24.3	84.2
optimized by mPWVWN/6-311G(2d)	**1**	321.9	1.735	1.847	1.829	1.838	104.2	105.1	84.2	−11.6
	1′	321.2	1.752	1.843	1.827	1.835	104.0	103.8	−81.3	−10.5
	2	319.5	1.739	1.817	1.832	1.825	103.0	103.7	−86.0	−31.2
	2′	312.0	1.739	1.855	1.838	1.847	99.8	104.9	50.3	−118.9
	3	313.6	1.739	1.851	1.830	1.841	100.7	103.7	8.3	−77.5
	3′	306.6	1.753	1.849	1.829	1.839	100.2	104.1	25.4	77.7
	4	313.6	1.750	1.843	1.825	1.834	100.7	104.2	3.4	−75.5
	4′	310.4	1.742	1.834	1.854	1.844	99.3	103.7	24.6	82.6

[a] X-ray results are from ref 13. ∠N−P−C−C_A are the dihedral angles of the two phenyl rings attached to each phosphorus atom. With respect to the other phosphorus atom, C_A and C_B are on the same sides of the N−P−C plane. But regarding the methylbenzyl group, C_A is on the same side, while C_B is on the opposite side. See Figure 1B for an example.

TABLE 3: R^2 Values for Correlations between Experimental NMR Chemical Shifts and Geometric Parameters

structure	δ^{expt} vs |sin∠N−P−C−C_A|, |sin∠N−P−C−C_B|	δ^{expt} vs |sin∠N−P−C−C_A|, |sin∠N−P−C−C_B|R_{P-N}	δ^{expt} vs |sin∠N−P−C−C_A|, |sin∠N−P−C−C_B|$^{av}R_{P-C}$
X-ray	0.880	0.880	0.894
Opt: B3LYP/6-31G(d)	0.867	0.963	0.884
Opt: B3LYP/6-311G(d)	0.867	0.967	0.882
Opt: mPW1PW91/6-31G(d)	0.869	0.957	0.901
Opt: BVWN5/6-311G(2d)	0.865	0.971	0.869
Opt: mPWVWN/6-311G(2d)	0.866	0.981	0.869

with this X-ray crystal structure, there is hardly any improvement that can be made. In addition, as shown in Table 3, there is basically no improvement in the shift-geometry correlations when either P−N bond length or the average P−C bond length was added in the regression. In contrast, local bond lengths around the phosphorus atoms were found to have important effects on the calculated NMR chemical shieldings/shifts in previous investigations of other phosphorus-containing systems.[14−16] These results suggest that while the overall conformations in this X-ray structure are good to reproduce the major part of experimentally observed chemical shift nonequivalence ($R^2 = 0.880$), the local bond lengths around the phosphorus atoms may need to be further refined. Previous investigations indicate that in some solid systems partial geometry optimization of the X-ray structure for the sites of interest is required to enable excellent predictions of spectroscopic properties including NMR shifts.[16,34−38]

Therefore, the next series of NMR calculations were performed with the structures of the phosphorus sites (phosphorus plus directly bonded atoms) being optimized while the remaining atoms in the molecule were fixed in their original crystal structural positions, to maintain the disordered environments (e.g., large variations of phenyl ring conformations) seen in the experiment. Indeed, as shown in the following section, this partial geometry optimization is able to recover the experimental chemical shift nonequivalence to an excellent level with $R^2 = 0.98$. Several computational methods were investigated on the geometry optimization, with the NMR shift predictions done by using the same, best method, GIAO-HF/6-311++G(2d,2p), from the above NMR calculations (Table 1).

We first used B3LYP/6-31G(d) for geometry optimization and indeed, as shown in Table 1, the R^2 is now improved to 0.945, a value similar to our previous calculations of ^{31}P chemical shifts in ordered solid molecular systems.[14] The SD

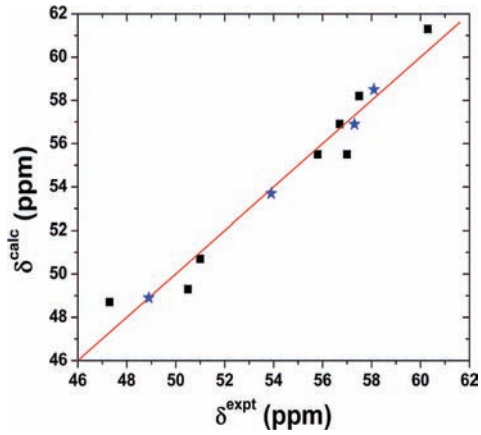

Figure 2. Plot of the calculated versus experimental ^{31}P NMR chemical shifts for the structure partially optimized by using the mPWVWN/6-311G(2d) method.

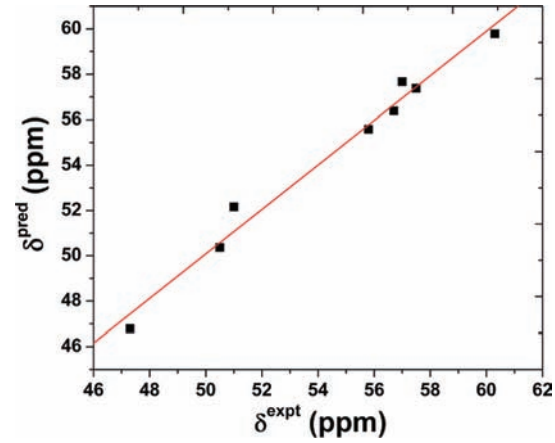

Figure 3. Plot of the predicted versus experimental ^{31}P NMR chemical shifts for the structure partially optimized by using mPWVWN/6-311G(2d) calculations. The predicted values were obtained from the regression eq 1.

is now dropped to 1.15 ppm, from 1.60 ppm when the original X-ray structure was used. This supports the hypothesis that the relatively poor performance of the calculations in the previous section is due to the poor structure for the phosphorus sites in this disordered system. It is interesting to note that with this optimized structure (Table S2, Supporting Information), the correlation between δ^{expt} and the two conformation angle terms plus the P−N bond length to have significantly improved with $R^2 = 0.963$, from 0.880 with the X-ray structure alone. This again supports the above hypothesis and the use of geometry optimization. The correlation result in Table 3 suggests that adding the P−C bond length information does not improve the correlation. This could be a result of the relatively longer bond lengths compared to P−N bonds (see Table 2 and in the Supporting Information Table S2) and thus a smaller impact on the phosphorus electron shielding effect, and/or that the P−C bond lengths (distances between the phosphorus atom and its attached phenyl rings) and both phenyl conformation angles are affected by the disorder in a very similar way and thus do not provide major new information. Regressions with more than three geometric parameters were abandoned due to overparametrization.

The same trends of improvement in NMR shift predictions and shift-geometry correlations were also observed with the optimizations with several other methods, as shown in Tables 1 and 3. These results further support the use of geometry optimization to interpret the experimental ^{31}P NMR chemical shifts in this disordered system. Comparisons among the data from using different quantum chemical methods nevertheless indicate different effects. Compared to the B3LYP method that contains a 20% Hartree−Fock exchange component,[17] the use of more Hartree−Fock exchange (25%) in another hybrid HF-DFT method mPW1PW91, which was found to yield good results of optimized geometries in other molecular systems,[30,39−42] actually results in reduction in performance in both NMR shift predictions (Table 1) and shift-geometry correlations (Table 3). Consistent with this observation of the effect of the HF exchange, the pure DFT methods (BVWN5 and mPWVWN) without any Hartree−Fock exchange produced better results. The best NMR shift predictions are from using the new pure DFT method mPWVWN, which is made by combining the modified Perdew−Wang 1991 (mPW) exchange functional[30] and VWN correlation functional.[33] This method results in $R^2 = 0.949$ and SD = 1.1 ppm, as illustrated in Figure 2 by square points. When the average of the two unassigned NMR shifts for each molecule is used (since the NMR experiment cannot give a definitive assignment for the two phosphorus atoms within the same molecule), the theory-versus-experiment correlation is even better, with $R^2 = 0.994$ and SD = 0.4 ppm. This is illustrated by the star points in Figure 2. Given the small range of experimental NMR data (13.0 ppm), this performance is quite good and similar to that of previous studies of ordered solids.[14]

The optimized structure from using the mPWVWN method also yields the best correlation between the experimental NMR chemical shifts and the geometric parameters. As illustrated in Figure 3, the predicted NMR chemical shifts from the following regression

$$\delta^{pred}(\text{ppm}) = 3.540|\sin\angle\text{N}-\text{P}-\text{C}-\text{C}_A|+ 14.06|\sin\angle\text{N}-\text{P}-\text{C}-\text{C}_B|+227.2R_{\text{P}-\text{N}} - 353.8 \quad (1)$$

have an excellent linear correlation ($R^2 = 0.981$) with the experimental data. The statistical p value for this regression is 0.00064. In contrast, the R^2 and p values for the regression of the two conformation terms alone are 0.866 and 0.0065, respectively. Therefore, both R^2 and p values indicate that the above three-parameter regression is better. This is consistent with the fact that each phosphorus atom is bonded to three groups: one nitrogen atom and two phenyl rings. This also suggests that all three bonding interactions around the phosphorus atoms are important in affecting the ^{31}P NMR chemical shifts.

Conclusions

The results we have described above are of interest for a number of reasons. First, these calculations give the first accurate predictions of the ^{31}P NMR chemical shifts in a disordered solid system with $R^2 = 0.95$ and SD = 1.1 ppm for an experimental range of 13.0 ppm, or with $R^2 = 0.994$ and SD = 0.4 ppm when the average of the two unassigned NMR shifts for each molecule is used. This is of interest in the context of structural elucidation for disordered solids of various chemical and biochemical systems. Second, our results indicate that geometry optimization gives the best accord with experiment for the structural investigation of NMR chemical shifts in the disordered system. Third, the structural origin of the experimentally observed NMR chemical shift nonequivalence in a disordered system was uncovered. The experimental ^{31}P NMR chemical shifts are mostly affected by the conformations of the two phenyl

rings that are attached to the phosphorus atoms. In addition, with the improved bond length from geometry optimization, the experimental NMR shifts can now be well correlated ($R^2 = 0.981$) with the three geometric parameters that reflect the interactions between each phosphorus atom and all of its three bonded groups. Taken together, these results should facilitate the use of quantum chemical methods for the structural characterization of the disordered solids and elucidation of NMR properties.

Acknowledgment. This work was supported in part by the NSF EPSCoR grant OIA-0556308 and NIH grant GM-085774. We are also grateful to the Mississippi Center of Supercomputing Research and USM Vislab for the generous use of their computing facilities. We thank Eric Oldfield and reviewers for helpful comments.

Supporting Information Available: The computed NMR chemical shieldings and optimized geometric parameters from using the B3LYP/6-31G(d), B3LYP/6-311G(d), mPW1PW91/6-31G(d), and BVWN5/6-311G(2d) methods (Tables S1 and S2). This material is available free of charge via the Internet at http://pubs.acs.org.

References and Notes

(1) Wasmer, C.; Lange, A.; Van Melckebeke, H.; Siemer, A. B.; Riek, R.; Meier, B. H. *Science* **2008**, *319*, 1523–1526.
(2) Petkova, A. T.; Ishii, Y.; Balbach, J. J.; Antzutkin, O. N.; Leapman, R. D.; Delaglio, F.; Tycko, R. *Proc. Natl. Acad. Sci. U.S.A.* **2002**, *99*, 16742–16747.
(3) Kern, T.; Hediger, S.; Muller, P.; Giustini, C.; Joris, B.; Bougault, C.; Vollmer, W.; Simorre, J. P. *J. Am. Chem. Soc.* **2008**, *130*, 5618–5619.
(4) Cadars, S.; Lesage, A.; Emsley, L. *J. Am. Chem. Soc.* **2005**, *127*, 4466–4476.
(5) Sakellariou, D.; Brown, S. P.; Lesage, A.; Hediger, S.; Bardet, M.; Meriles, C. A.; Pines, A.; Emsley, L. *J. Am. Chem. Soc.* **2003**, *125*, 4376–4380.
(6) Hedin, N.; Graf, R.; Christiansen, S. C.; Gervais, C.; Hayward, R. C.; Eckert, J.; Chmelka, B. F. *J. Am. Chem. Soc.* **2004**, *126*, 9425–9432.
(7) Kaji, H.; Schmidt-Rohr, K. *Macromolecules* **2002**, *35*, 7993–8004.
(8) Clark, T. M.; Grandinetti, P. J. *J. Phys.: Condens. Matter* **2003**, *15*, S2387–S2395.
(9) de Dios, A. C.; Pearson, J. G.; Oldfield, E. *Science* **1993**, *260*, 1491–1496.
(10) Sun, H. H.; Sanders, L. K.; Oldfield, E. *J. Am. Chem. Soc.* **2002**, *124*, 5486–5495.
(11) Cheng, F.; Sun, H. H.; Zhang, Y.; Mukkamala, D.; Oldfield, E. *J. Am. Chem. Soc.* **2005**, *127*, 12544–12554.
(12) Mukkamala, D.; Zhang, Y.; Oldfield, E. *J. Am. Chem. Soc.* **2007**, *129*, 7385–7392.
(13) Robert, F.; Gimbert, Y.; Averbuch-Pouchot, M. T.; Greene, A. E. *Z. Kristallogr.-New Cryst. Struct.* **2000**, *215*, 233–236.
(14) Zhang, Y.; Oldfield, E. *J. Phys. Chem. B* **2004**, *108*, 19533–19540.
(15) Zhang, Y.; Oldfield, E. *J. Phys. Chem. B* **2006**, *110*, 579–586.
(16) Mao, J. H.; Mukherjee, S.; Zhang, Y.; Cao, R.; Sanders, J. M.; Song, Y. C.; Zhang, Y. H.; Meints, G. A.; Gao, Y. G.; Mukkamala, D.; Hudock, M. P.; Oldfield, E. *J. Am. Chem. Soc.* **2006**, *128*, 14485–14497.
(17) Becke, A. D. *J. Chem. Phys.* **1993**, *98*, 5648–5652.
(18) Lee, C.; Yang, W.; Parr, R. G. *Phys. Rev. B* **1988**, *37*, 785–789.
(19) Ditchfield, R. *Mol. Phys.* **1974**, *27*, 789–807.
(20) Cheeseman, J. R.; Trucks, G. W.; Keith, T. A.; Frisch, M. J. *J. Chem. Phys.* **1996**, *104*, 5497–5509.
(21) Frisch, M. J.; Trucks, G. W.; Schlegel, H. B.; Scuseria, G. E.; Robb, M. A.; Cheeseman, J. R.; Montgomery, J. A., Jr.; Vreven, T.; Kudin, K. N.; Burant, J. C.; Millam, J. M.; Iyengar, S. S.; Tomasi, J.; Barone, V.; Mennucci, B.; Cossi, M.; Scalmani, G.; Rega, N.; Petersson, G. A.; Nakatsuji, H.; Hada, M.; Ehara, M.; Toyota, K.; Fukuda, R.; Hasegawa, J.; Ishida, M.; Nakajima, T.; Honda, Y.; Kitao; O.; Nakai, H.; Klene, M.; Li, X.; Knox, J. E.; Hratchian, H. P.; Cross, J. B.; Bakken, V.; Adamo, C.; Jaramillo, J.; Gomperts, R.; Stratmann, R. E. ; Yazyev, O.; Austin, A. J.; Cammi, R.; Pomelli, C.; Ochterski, J. W.; Ayala, P. Y.; Morokuma, K.; Voth, G. A.; Salvador, P.; Dannenberg, J. J.; Zakrzewski, V. G.; Dapprich, S.; Daniels, A. D.; Strain, M. C.; Farkas, O.; Malick, D. K.; Rabuck, A. D.; Raghavachari, K.; Foresman, J. B.; Ortiz, J. V.; Cui, Q.; Baboul, A. G.; Clifford, S.; Cioslowski, J.; Stefanov, B. B.; Liu, G.; Liashenko, A.; Piskorz, P.; Komaromi, I.; Martin, R. L.; Fox, D. J.; Keith, T.; Al-Laham, M. A.; Peng, C. Y.; Nanayakkara, A.; Challacombe, M.; Gill, P. M. W.; Johnson, B.; Chen, W.; Wong, M. W.; Gonzalez, C.; Pople, J. A. *Gaussian 03*, Revision D.01; Gaussian, Inc., Wallingford, CT, 2004.
(22) Frisch, M. J.; Trucks, G. W.; Schlegel, H. B.; Scuseria; G. E.; Robb, M. A.; Cheeseman, J. R.; Zakrzewski, V. G.; Montgomery, J. A., Jr.; Stratmann, R. E.; Burant; J. C.; Dapprich; S.; Millam, J. M.; Daniels, A. D.; Kudin, K. N.; Strain, M. C.; Farkas, O.; Tomasi, J.; Barone, V.; Cossi, M.; Cammi, R.; Mennucci, B.; Pomelli, C.; Adamo, C.; Clifford, S.; Ochterski, J.; Petersson, G. A.; Ayala, P. Y.; Cui, Q.; Morokuma, K.; Malick, D. K.; Rabuck; A. D.; Raghavachari, K.; Foresman, J. B.; Cioslowski, J.; Ortiz, J. V.; Baboul, A. G.; Stefanov, B. B.; Liu, G.; Liashenko, A.; Piskorz, P.; Komaromi, I.; Gomperts, R.; Martin, R. L.; Fox, D. J.; Keith, T.; Al-Laham, M. A.; Peng, C. Y.; Nanayakkara, A.; Challacombe, M.; Gill, P. M. W.; Johnson, B.; Chen, W.; Wong, M. W.; Andres, J. L.; Gonzalez, C.; Head-Gordon, M.; Replogle, E. S.; Pople, J. A. *Gaussian 98*, Revision A.9; Gaussian, Inc., Pittsburgh, PA, 1998.
(23) de Dios, A. C.; Oldfield, E. *Chem. Phys. Lett.* **1993**, *205*, 108–116.
(24) Dedios, A. C.; Laws, D. D.; Oldfield, E. *J. Am. Chem. Soc.* **1994**, *116*, 7784–7786.
(25) Cossi, M.; Barone, V.; Cammi, R.; Tomasi, J. *Chem. Phys. Lett.* **1996**, *255*, 327–335.
(26) Cossi, M.; Scalmani, G.; Rega, N.; Barone, V. *J. Chem. Phys.* **2002**, *117*, 43–54.
(27) Cances, E.; Mennucci, B.; Tomasi, J. *J. Chem. Phys.* **1997**, *107*, 3032–3041.
(28) Mennucci, B.; Tomasi, J. *J. Chem. Phys.* **1997**, *106*, 5151–5158.
(29) Cossi, M.; Barone, V.; Mennucci, B.; Tomasi, J. *Chem. Phys. Lett.* **1998**, *286*, 253–260.
(30) Adamo, C.; Barone, V. *J. Chem. Phys.* **1998**, *108*, 664–675.
(31) Perdew, J. P.; Burke, K.; Wang, Y. *Phys. Rev. B* **1996**, *54*, 16533–16539.
(32) Becke, A. D. *Phys. Rev. A* **1988**, *38*, 3098–3100.
(33) Vosko, S. H.; Wilk, L.; Nusair, M. *Can. J. Phys.* **1980**, *58*, 1200–1211.
(34) McMahon, M. T.; deDios, A. C.; Godbout, N.; Salzmann, R.; Laws, D. D.; Le, H. B.; Havlin, R. H.; Oldfield, E. *J. Am. Chem. Soc.* **1998**, *120*, 4784–4797.
(35) Zhang, Y.; Gossman, W.; Oldfield, E. *J. Am. Chem. Soc.* **2003**, *125*, 16387–16396.
(36) Zhang, Y.; Oldfield, E. *J. Am. Chem. Soc.* **2004**, *126*, 9494–9495.
(37) Zhang, Y.; Oldfield, E. *J. Am. Chem. Soc.* **2004**, *126*, 4470–4471.
(38) Zhang, Y.; Oldfield, E. *J. Am. Chem. Soc.* **2008**, *130*, 3814–3823.
(39) Yang, J.; Huang, S. X.; Zhao, Q. S. *J. Phys. Chem. A* **2008**, *112*, 12132–12139.
(40) Xu, B.; Li, Q. S.; Xie, Y. M.; King, R. B.; Schaefer, H. F. *Inorg. Chem.* **2008**, *47*, 6779–6790.
(41) Zhang, Y.; Lewis, J. C.; Bergman, R. G.; Ellman, J. A.; Oldfield, E. *Organometallics* **2006**, *25*, 3515–3519.
(42) Zhang, Y.; Guo, Z. J.; You, X. Z. *J. Am. Chem. Soc.* **2001**, *123*, 9378–9387.

JP9001324